



Published in final edited form as:

*Neurobiol Aging*. 2012 March ; 33(3): 623.e15–623.e24. doi:10.1016/j.neurobiolaging.2011.03.002.

## Dopamine and fronto-striatal networks in cognitive aging

Ellen C. Klostermann<sup>a,b</sup>, Meredith N. Braskie<sup>a</sup>, Susan M. Landau<sup>a,b</sup>, James P. O'Neil<sup>b</sup>, and William J. Jagust<sup>a,b</sup>

<sup>a</sup>Helen Wills Neuroscience Institute, University of California Berkeley, Berkeley, CA 94720-3190, USA

<sup>b</sup>Life Sciences Division, Lawrence Berkeley National Laboratory, Berkeley, CA 94720, USA

### Abstract

Recent studies have linked dopamine to differences in behavior and brain activity in normal individuals. We explored these relationships in older and younger adults by investigating how functional connectivity between the striatum and prefrontal cortex is related to caudate dopamine and verbal working memory task performance. We studied 12 young and 18 older participants with functional magnetic resonance imaging (fMRI) during this task, and used positron emission tomography with the tracer 6-[<sup>18</sup>F]-fluoro-L-*m*-tyrosine (FMT) to assess dopamine synthesis capacity. Younger adults had a greater extent of frontal-caudate functional connectivity during the load-dependent delay period of the working memory task than the older participants. Across all subjects, the extent of this functional connectivity was negatively correlated with dopamine synthesis capacity, such that participants with the greatest connectivity had the lowest caudate FMT signal. Additionally, the extent of functional connectivity was positively correlated with working memory performance. Overall these data suggest interdependencies exist between fronto-striatal functional connectivity, dopamine, and working memory performance and that this system is functioning suboptimally in normal aging.

### Keywords

aging; working memory; dopamine; functional connectivity; FMT

## 1. Introduction

Dopamine may influence prefrontal cortex (PFC) function either directly via a dopaminergic mesocortical pathway from the ventral tegmental area (VTA), or through striato-thalamocortical loops that are themselves modulated by the dopaminergic nigrostriatal pathway. Alterations in PFC function have been linked to changes in both of these dopamine systems. For example, striato-thalamo-cortical loops are functionally relevant, support a variety of cognitive and motor behaviors, and are particularly important for tasks that involve executive function (Alexander et al., 1986; Alexander and Crutcher, 1990; Lehericy et al., 2004; for review, see Middleton and Strick, 2000). In addition, depletion of dopamine

© 2011 Elsevier Inc. All rights reserved.

**Correspondence to:** Ellen C. Klostermann, Helen Wills Neuroscience Institute, 132 Barker Hall, MC#3190, Berkeley, CA 94720-3190, USA, Phone: (510)643-6616 Fax: (510)643-4966, eklostermann@berkeley.edu.

**Publisher's Disclaimer:** This is a PDF file of an unedited manuscript that has been accepted for publication. As a service to our customers we are providing this early version of the manuscript. The manuscript will undergo copyediting, typesetting, and review of the resulting proof before it is published in its final citable form. Please note that during the production process errors may be discovered which could affect the content, and all legal disclaimers that apply to the journal pertain.

Disclosure Statement: There are no actual or potential conflicts of interest.

in the dorsolateral prefrontal cortex (DLPFC) causes impairment in delayed attention task performance that is equivalent to the impairment seen with surgical ablation of this region (Brozoski et al., 1979). Effects of dopamine are particularly notable during the delay period of working memory tasks during which encoded information is actively kept in mind (Williams and Goldman-Rakic, 1995).

Post mortem studies of human aging show that nigral dopaminergic neurons are lost at a rate of 5–10% per decade (Fearnley and Lees, 1991; Ma et al., 1999), a figure that corresponds well with *in vivo* PET results that report loss of dopamine transporters (DAT) (Volkow et al., 1994), and vesicular monoamine transporters (VMAT2) of around 8% per decade (Frey et al., 1996). These changes are accompanied by a decrease in the number of dopaminergic binding sites in the caudate (Severson et al., 1982), a decline in the number of D<sub>1</sub> and D<sub>2</sub> receptors in the striatum (Seeman et al., 1987; Rinne et al., 1990), and a decline in the number of D<sub>2</sub> and D<sub>3</sub> receptors in extrastriatal regions, particularly in the frontal cortex (Kaasinen et al., 2000). In contrast, studies of changes in dopamine synthetic enzymes using both PET ligands during life and post-mortem assays have not consistently shown reductions, suggesting that dopamine synthesis might be upregulated as an age-related compensatory mechanism (Wolf et al., 1991; Kish et al., 1995). In line with these findings, we have recently reported strong PET evidence for increased dopamine synthesis capacity with aging (Braskie et al., 2008).

Variability in striatal dopamine function is linked to differences in both behavior and brain activity in normal individuals (Backman et al., 2000; Tomasi et al., 2009), and patients with Parkinson's disease (Gabrieli et al., 1996; Kensinger et al., 2003; Lewis et al., 2003, 2005; Zgaljardic et al., 2004; Moustafa et al., 2008). Hence it is reasonable to suppose that this neurochemical change could underlie aspects of age-related cognitive decline (Backman et al., 2010). Many behavioral studies have revealed declines in both general measures of executive function and specific performance in working memory with advancing age (Park et al., 1996; Park and Hedden, 2002; Reuter-Lorenz and Sylvester, 2004). While structural changes in PFC have been proposed to underlie some of these behavioral effects (Raz et al., 1997), there is also considerable evidence for alterations in brain functions that support working memory performance (Rypma and D'Esposito, 2000; Nagel et al., 2010). Since aging thus involves both profound neurochemical alterations in the dopaminergic system, and changes in brain activity during working memory, the investigation of how these phenomena are related to one another and to age-related behavioral decline is an important topic.

We have previously reported that during the load-dependent delay period of a working memory task, caudate dopamine synthesis in older adults was positively correlated with working memory capacity and fMRI activity in the inferior frontal junction (IFJ; BA 44/6) (Landau et al., 2009). This study, however, did not specifically evaluate differences between older and younger adults. An important methodological consideration in such aging studies is the effect of atrophy, since, in addition to PFC, striatal atrophy is a well-characterized effect of aging (Gunning-Dixon et al., 1998; Raz et al., 2003). Our initial investigation of the effect of aging on brain activation and behavior used atrophy-corrected measures of striatal dopamine function, and reported that dopamine synthesis capacity was associated with fMRI deactivation in the posterior cingulate cortex and precuneus in younger adults (Braskie et al., 2010). In the current study, we investigated how age effects in the dopamine system underlie behavioral and functional brain changes, by specifically targeting striato-frontal networks. This approach is unique in utilizing both atrophy corrected measures of striatal dopamine function and a multivariate approach to functional MRI data. Our specific hypothesis was based upon anatomical connectivity patterns through which striatum influences PFC function. Thus, we aimed to demonstrate how the functional connectivity between the

frontal lobe and striatum in older and younger adults during the delay period of a working memory task relates to individual differences in dopamine synthesis capacity and working memory task performance.

## 2. Method

### 2.1 Participants

Twelve younger adults and eighteen older adults participated in the experiment (see Table 1). All participants underwent tests of executive function, working memory, language, episodic verbal and spatial memory, motor response, and general cognitive function. Participants were excluded from the study if they scored below a 26 on the Mini Mental State Exam (MMSE), had a Geriatric Depression Rating (21 item) score greater than 10, or scored below low average for their age on the Wechsler Memory Scale (WMS), auditory immediate age-adjusted summed score (the WMS logical memory immediate score and WMS verbal paired associates immediate score), or Wechsler Adult Intelligence Digit Span age-adjusted score (which includes Digit Span Forward and Digit Span Backward). Participants were also excluded from the study if they were current smokers, hypertensive, taking medication that could affect dopamine function or cognition, or had a history of neurological or psychological disorders, serious head injury, drug or alcohol abuse, or major systemic disease.

The older adults were significantly more educated, reflecting the fact that many participants in the younger adult group were still college students (Mann-Whitney two-tailed test  $p < 0.0001$ ). The older adult group's MMSE scores did not significantly differ from those of the younger adults. All of the 30 participants in this study were reported on in two previous studies (Braskie et al., 2008; Braskie et al., 2010). Additionally, seventeen of the older adult participants were reported on in another study (Landau et al., 2009). Informed consent was obtained from all participants in accordance with the policies of the University of California, Berkeley.

### 2.2 Behavioral methods & stimuli

Participants completed a modified version of the Sternberg delayed recognition task (Sternberg, 1966). During the task, participants first encoded sets of 2, 4, or 6 letters for 4 seconds. After a delay period of 12 seconds during which participants focused on a "+", participants were shown a probe letter for 2 seconds. Participants pressed one button if the letter was a member of the set of letters they had encoded, and another button if it was not a member of the letter set. Each trial was followed by a jittered inter-stimulus interval (ISI) of 8–12 seconds. The experiment consisted of six, 7-minute long experimental runs, each containing 15 trials (5 trials for each letter load; letter load order randomized across runs). Different sets of letters were used for each trial both within and across the six runs. All stimuli were presented using E-prime software (Psychology Software Tools, Inc, Pittsburgh, PA; <http://www.pstnet.com>). The stimuli were back-projected onto a screen mounted at the participant's chest level, which was viewed using an angled mirror placed inside the head coil. Button responses were made on a nonmagnetic response box designed for use in the MRI environment. Sternberg task accuracy was calculated as the total number of correct trials, divided by the total number of possible trials. Reaction time (RT) for this task was calculated as the average RT for all responses.

### 2.3 fMRI methods

Participants were scanned within six months of their PET scans in a 4T Varian Inova scanner (Varian Inc., Palo Alto, CA) using a 2-shot gradient echo, echo-planar imaging (EPI) sequence (18 slices; TR/shot= 1.0 sec, TE=28 ms, flip angle 20°, 64 × 64 [3.5 × 3.5

mm] in-plane resolution, FOV = 224 × 224). The scanning session consisted of 6 functional runs, each consisting of 414 time points.

A gradient-echo multislice (GEMS) sequence using the same 18 slices defined for the EPI scans was used to aid in the coregistration of the fMRI scans to the standard MNI brain (FOV = 224 × 224; TR = 200 ms; TE = 5 ms). A 3D T1-weighted magnetization prepared fast low angle shot (MPFLASH) scan (1.55 mm slices, no slice gap; 256 × 256 [.875 × .875 mm] in-plane resolution; FOV = 224 × 224; TR = 9 ms; TE = 5 ms) was acquired for each participant so that partial volume correction of PET scans and region of interest demarcation could be performed.

## 2.4 PET data acquisition

PET scanning was performed using the tracer 6-[<sup>18</sup>F]-fluoro-L-*m*-tyrosine (FMT). This tracer is similar to [<sup>18</sup>F]Fluorodopa, although because it is neither a substrate for catechol-O-methyltransferase nor the vesicular monoamine transporter, its PET signal more specifically reflects the activity of aromatic amino acid decarboxylase (AADC). Thus, FMT is a good indicator of the ability of presynaptic dopaminergic neurons to synthesize dopamine when provided with adequate substrate (Jordan et al., 1997; DeJesus et al., 2001). FMT was synthesized at Lawrence Berkeley National Laboratory using the procedure described in VanBrocklin et al. (2004). Participants ingested 2.5 mg/kg of carbidopa approximately one hour prior to scanning to minimize the peripheral metabolism of FMT. A Siemens ECAT EXACT HR PET scanner in 3D acquisition mode was used to acquire the PET scans (45 parallel slices; 4 mm thick; 3.6 mm in-plane voxel size). A transmission scan lasting 10 min was obtained for attenuation correction. This scan was followed by a bolus injection of 2.0–3.0 mCi of FMT into the antecubital vein. Next, a dynamic acquisition sequence in 3D mode was obtained: 4 × 1 min, 3 × 2 min, 3 × 3 min, and 14 × 5 min (89 min total scan time). The data were reconstructed using an ordered subset expectation maximization (OSEM) algorithm (image size 256 × 256, 6 iterations with 16 subsets). Scatter correction and a 6 mm full width at half maximum Gaussian filter were applied to the data. We ensured that subject motion was minimal and adequate count rates were obtained.

## 2.5 PET reference region

A cerebellar reference region was chosen because this region is essentially devoid of tracer uptake due to lack of dopamine terminals, resulting in a brain region with only non-specific accumulation of tracer. Cerebellar masks including two thirds of the slices posterior to the last slice in which the superior cerebellar peduncles stretched superiorly were manually drawn on the coronal plane of each participant's structural MRI image. The inclusion of only these posterior slices ensured that the reference region was not contaminated by the FMT signal from the substantia nigra and ventral tegmental area. To exclude large white matter tracts, cerebellar segmentation was then done automatically using the "FSL Automatic Segmentation Tool" (FAST) software (Zhang et al., 2001) from version 3.3 of the "Analysis Group at the Oxford Centre for Functional MRI of the Brain" (FMRIB) software library (FSL). As previously reported, the striatal signal differences between the two age groups were not affected by the FMT signal in the cerebellum (Braskie et al., 2008).

## 2.6 PET analysis methods

Each PET frame was realigned to the summed image of the first ten frames using Statistical Parametric Mapping (SPM2; Wellcome Department of Cognitive Neurology, London) to adjust for between-frame subject motion. Each participant's MRI scans, brain matter masks, and cerebellar grey matter masks were coregistered to their respective summed PET images.  $K_i$  images were created from PET frames corresponding to 24 to 89 min using Patlak

graphical analysis for irreversible binding (Patlak and Blasberg, 1985). The PET reference regions were defined by the individual cerebellar grey matter masks.

## 2.7 Partial volume correction

In order to account for the effects of brain atrophy that may accompany aging, we performed a correction for partial volume effects. As previously described (Meltzer et al., 1999), a two-compartment model was used for the partial volume correction. In short, the PET scanner point spread function (which was derived empirically from our scanner) was applied to the brain matter binary mask by convolving the MRI brain matter mask with a Gaussian kernel. The observed PET scan was divided by the convolved brain matter mask to yield the corrected PET scan (Meltzer et al., 1999). The FMT signal values reported in this study are therefore all partial volume corrected (PVC) for cerebrospinal fluid contamination of PET voxels. To calculate  $K_i$  values for the right dorsal caudate, ROIs for that region were drawn as in Braskie et al. (2008).

## 2.8 fMRI univariate analysis

The fMRI data were analyzed using SPM2 software (Wellcome Department of Cognitive Neurology, London, UK). It was ensured during the realignment procedure in SPM2 that movements greater than 3 mm or 3 degrees did not occur during the experiment. The data were first reconstructed into SPM2 image files and interpolated to a TR of 1.0 using a linear time interpolation algorithm, doubling the effective sampling rate (Noll et al., 1999). Functional and anatomical images were recalibrated, such that the origin of all images was fixed to the anterior commissure. The functional images were then realigned, using the first functional image acquired as the reference. The images were then smoothed using an 8 mm FWHM smoothing kernel. The covariates were entered into the general linear model (GLM) using the following structure: the first covariate occurred at the onset of the encoding epoch (first TR, 0 sec), a second covariate at the third TR modeled late encoding-related activity (4 sec). This late covariate was included to reduce noise in the estimate of the baseline because encoding processes could continue into the delay period. Early and late delay period phases were modeled with covariates at the fifth and seventh TRs (8 and 12 seconds, respectively). The delay effects in this study represent the sum of the early and late delay covariates ((High Load Delay Early + High Load Delay Late) – (Low Load Delay Early + Low Load Delay Late)). The response epoch was modeled with a covariate at the ninth TR (16 sec). A GLM was run using 16 conditions of interest (Low Load Trials: encoding early, encoding late, delay early, delay late, response; Medium Load Trials: encoding early, encoding late, delay early, delay late, response; High Load Trials: encoding early, encoding late, delay early, delay late, response; incorrect trials) as regressors. A high-pass filter removed frequencies below 0.01 Hz in the data. The individual subject contrasts were computed using a fixed-effects analysis, which collapsed across the 6 fMRI runs. Each participant's GEMS scan was coregistered to the MPFLASH scan. Normalization took place in two steps. First, the coregistered MPFLASH was normalized to the MNI standard brain in SPM2. Then, the resulting transformed anatomical file was used to normalize the contrast maps. Group statistics (t-tests) were then performed on the experimental contrasts using a threshold of  $p < 0.05$ , FDR corrected with a 10 voxel extent. Group level random-effects analyses were performed on the load-dependent encoding, delay, and response period data. This allowed for the identification of regions that had significant fMRI activity in response to increasing working memory load during the three stages of the working memory task. Neurological convention was employed for all figures.

## 2.9 Beta series correlation analysis

Because BA 44/6 has previously been related to dopamine synthesis in the caudate (Landau et al., 2009), this region was chosen to be our seed region in the functional connectivity

analysis. While activity left BA 44/6 was observed in the Landau et al. study that used only older adult participants, significant activity was found in the right hemisphere in this study for the load-dependent delay period contrast when participants were collapsed across age group. This laterality difference may reflect age-related asymmetry reductions in prefrontal fMRI activity often observed during working memory tasks (Dolcos et al., 2002; Reuter-Lorenz, 2002). The identification of a seed region active across both participant groups was necessary for this method of connectivity analysis. Thus, the seed region in our study was in right IFJ (BA 44/6).

A beta series correlation analysis was performed as described in Rissman et al. (2005). This multivariate analysis method has previously been shown to be successful in characterizing discrete patterns of functional connectivity for the three phases of a typical working memory task (Rissman et al., 2005; Gazzaley et al., 2004). The ~10 most active voxels in right Brodmann's Area (BA) 44/6 for each individual participant in the load dependent delay contrast (high load delay > low load delay) were selected using xjview software (<http://www.alivelearn.net/xjview/>). These 10-voxel masks were then used as seeds for the connectivity analysis.

We performed connectivity analysis using this right IFJ (BA 44/6) seed on data for the high load>low load contrast for all three phases of the working memory task: 1) the load-dependent delay period, 2) the load-dependent encoding period, and 3) the load-dependent response period. We chose to concentrate our analyses on the load-dependent delay period, given the importance of dopamine during the delay period of working memory tasks. The connectivity analyses performed for the load-dependent encoding and response phase data were meant to serve as controls for the delay period analysis.

To perform the connectivity analyses, a GLM using a covariate structure identical to that described for the univariate analysis was run. Specifically, in each trial (which was either a low, medium, or high load trial) there were 5 stages (encoding early, encoding late, delay early, delay late, response). Each stage of each trial was coded as 1 of 15 possible individual covariates (Low Load Trials: encoding early, encoding late, delay early, delay late, response; Medium Load Trials: encoding early, encoding late, delay early, delay late, response; High Load Trials: encoding early, encoding late, delay early, delay late, response) and entered into the GLM. A high-pass filter removed frequencies below 0.01 Hz in the data. The GLM resulted in parameter estimates, or *beta values*, for all 5 task stages for all 90 trials in the experimental task (450 total beta values). The beta values were then sorted by trial type and task stage, resulting in 15 *beta series*, one for each possible covariate.

Next, correlation maps were obtained such that the activity in the seed voxels during each load-dependent period (delay, encoding, and response) was correlated with activity in all other brain voxels during that same period. These analyses included data from all fMRI runs. These whole brain correlation maps were then arc-hyperbolic tangent transformed so that the distribution of the correlation values (-1 to 1) approached that of a normal distribution. Next, these values were z-transformed (z-transformed correlation coefficient =  $\text{atanh transformed correlation coefficient} / (1/\sqrt{N-3})$ , where N=the number of data points used to calculate the correlation coefficient). The resulting z-score maps were normalized to MNI space using SPM2. Group level random effects t-tests were then performed on these z-score maps to identify brain areas that were significantly correlated with the right BA 44/6 seed during the load-dependent delay, encoding, and response phases.

To measure the extent of functional connectivity between BA 44/6 and the caudate, the number of voxels above a threshold of  $p=0.05$  in a caudate region of interest (ROI) for each participant were counted. This caudate ROI was taken from the WFU Pickatlas

(<http://www.fmri.wfubmc.edu/cms/software#PickAtlas>). These extent values were related to FMT signal in the right caudate and task performance using Pearson correlations for the older and younger adults together. If a measure of the strength of connectivity between the seed region and the right caudate (the highest t-value in each participant's right caudate in the load-dependent delay period connectivity map) was used instead of the connectivity extent measure, similar relationships between strength of connectivity and FMT, and strength of connectivity and task accuracy were observed. This strength of connectivity measure was also significantly correlated with the connectivity extent measure ( $r=0.72$ ,  $p<0.01$ ). A two-tailed  $\alpha$  value of  $p<0.05$  was used for all connectivity analyses.

### 3. Results

#### 3.1 Behavioral and FMT results

Participant characteristics are shown in Table 1. Eighteen older adults (average age 64.8 years; 12 female) and twelve younger adults (average age 22.7 years; 9 female) participated in the study. As previously reported (Braskie et al., 2008), older adults had significantly higher FMT signal in the right ( $t(28)=2.47$ ,  $p=.02$ ) and left ( $t(28)=2.87$ ,  $p=.01$ ) caudate than younger adults. There was a trend for the average percent accuracy in the working memory task to be significantly higher for the younger adults than the older adults ( $t(28)=-1.82$ ,  $p=0.079$ ). Older adults were on average significantly slower than younger adults to make their memory judgments in the response phase ( $t(28)=2.55$ ,  $p=0.017$ ).

#### 3.2 Univariate fMRI results

For the purposes of this study, we were particularly interested in fMRI activity across all participants during the load-dependent delay period of the task (high load delay period > low load delay period). Regions active during the load-dependent delay period across both groups are shown in Supplemental Table 1. Significant activation in right BA 44/6 ( $x=64$ ,  $y=18$ ,  $z=32$ ) was found in this contrast (Figure 1A). Because BA 44/6 has previously been related to dopamine synthesis in the caudate (Landau et al., 2009), this frontal region was used as the seed region for further connectivity analyses.

#### 3.3 Functional connectivity, FMT, and accuracy data

We performed a beta series correlation analysis in order to identify regions whose fMRI activity is correlated with that of the right BA 44/6 during 1) the load-dependent encoding period, 2) the load-dependent delay period, and 3) the load-dependent response period. The encoding and response phase analyses were meant to serve as controls for the delay period analysis. The average seed region for functional connectivity analysis, defined from each participant's load-dependent delay period, is shown in Figure 1B. Caudate regions functionally correlated with right BA 44/6 for younger and older adults during the load-dependent encoding, delay and retrieval periods are shown in Figure 2. Functional MRI activity in right BA 44/6 was significantly correlated with activity in the right caudate during the load-dependent encoding and delay periods only in younger adults, and with fMRI activity in bilateral caudate during the load-dependent response period in both older and younger adults. Other regions with fMRI activity that was significantly correlated with BA 44/6 during the load-dependent delay period for younger and older adults are shown in Supplemental Tables 2 and 3, respectively.

The number of voxels above a threshold of  $p=0.05$  in a right caudate ROI of each participant were counted and represented the extent of functional connectivity between BA 44/6 and the right caudate. The extent of connectivity during the load-dependent delay period was significantly greater in younger adults than older adults ( $t(28)=-2.972$ ,  $p<0.006$ ) (see Figure 3). During the load-dependent encoding and response phases, however, the extent of

connectivity in the right caudate did not significantly differ between younger and older adults (load-dependent encoding phase,  $t(28)=-1.26$ ,  $p=0.22$ ; load-dependent response phase,  $t(28)=-0.702$ ,  $p=0.49$ ).

The relationship between the extent of functional connectivity in the right caudate during all three load-dependent phases of the working memory task and right caudate FMT was explored. When the participants were collapsed across age group, there was a significant negative correlation between FMT in the caudate and connectivity extent during the load-dependent delay period ( $r=-0.472$ ,  $p<0.01$ ) (see Figure 4). Importantly, there was not a significant relationship between FMT in the caudate and extent values during the load-dependent encoding ( $r=-0.264$ ) and response ( $r=-0.203$ ) periods.

When participants were collapsed across age group, there was a significant positive correlation between task accuracy and the extent of connectivity between BA 44/6 and the right caudate during the load-dependent delay period ( $r=0.400$ ,  $p<0.05$ ) (see Figure 5), such that participants with a greater extent of frontal-caudate functional connectivity performed better on the working memory task.

#### 4. Discussion

In this study, we examined the degree of frontal-striatal functional connectivity during a working memory task in older and younger adults. When the two age groups were compared, younger adults had a significantly greater extent of functional connectivity between the right IFJ (BA 44/6) and the right caudate during the delay period, but not during the encoding or response periods. The extent of functional connectivity in the right caudate was, in turn, negatively correlated with caudate FMT signal, again only during the delay period of the task. Furthermore, across all participants, the extent of functional connectivity in the right caudate was positively correlated with working memory task performance. The negative relationship between dopamine synthesis and connectivity, and the positive relationship between connectivity and task performance supports the view that higher dopamine synthesis is associated with non-optimal function of this neural system in aging (Braskie et al., 2008).

Activity in the IFJ region in the frontal lobe (BA 44/6) active in this study has previously been seen during a similar working memory task (Hester and Garavan, 2004). This region has also been related to caudate FMT signal and task accuracy in a subset of the same participants (Landau et al., 2009). The IFJ has been associated with the integration of stimulus maintenance and motor preparation, likely required during the delay period of the working memory task. In this study, the reduced functional connectivity between this region and the right caudate is related to poorer performance on the working memory task. These data suggest that a reduction in these regions' ability to work together to maintain a stimulus during the delay period may cause an increase in the number of errors made during the response phase of the task.

Age-related declines in working memory function have previously been observed, particularly for tasks with higher processing demands (for review, see Reuter-Lorenz and Sylvester, 2004). In many studies, older adults are slower and less accurate during working memory tasks than younger adults. Along with these behavioral changes, the neural circuitry of working memory changes with age. While many regions show activity patterns that are similar for both groups, greater bilateral PFC activation is often observed for older adults in studies where PFC unilateral activity is found for younger adults (Cabeza et al., 2002). Better working memory performance has been associated with this additional PFC activity, suggesting that overactivation may serve a compensatory function in older adults (Rypma



and D'Esposito, 2001; for review, see Reuter-Lorenz, 2002). In our study, the right IFJ effect in the load-dependent delay contrast was significantly greater in the older adult group, though both age groups did exhibit significant fMRI activity in this region.

Previous studies have found that changes in the dopamine system are related to deficits on a wide range of cognitive tasks. In a study that investigated the relationship between D<sub>2</sub> binding and neuropsychological tests of perceptual speed and episodic memory, D<sub>2</sub> binding accounted for more variation in performance than chronological age (Backman et al., 2000). Low levels of striatal dopamine transporter (DAT) in older adults have been linked to impairments in episodic and executive functioning (Erixon-Lindroth et al., 2005). Declines in brain dopamine levels with age have been related to a decline in performance on motor tasks and frontal lobe tasks (e.g., the Stroop task) (Volkow et al., 1998). Furthermore, age-related reductions in D<sub>1</sub> binding have been related to the under-recruitment of brain regions involved in working memory (Backman et al., 2009). Here, non-optimal levels of caudate FMT were associated with reduced functional connectivity, which was related to decreased working memory performance.

It is important to note that the group difference in caudate FMT signal in our study does not indicate that older adults have higher caudate dopamine levels than younger adults (Braskie et al., 2008). Because the FMT radiotracer used in this study is a substrate of AADC, a dopamine-synthesizing enzyme that converts levodopa to dopamine, higher FMT signal is instead reflective of an increase in dopamine synthesis capacity in the caudate in older adults. This increase in synthesis capacity may fail to adequately compensate for other age-related changes taking place in this neurochemical system (Wolf et al., 1991; Kish et al., 1995).

A previous study using the same functional connectivity method found a delay period network similar to the one identified in our study (Gazzaley et al., 2004). Using a seed in the fusiform face area (FFA), Gazzaley and colleagues (2004) identified a network of regions supporting the maintenance of face stimuli including dorsolateral and ventrolateral PFC, the premotor cortex, the intraparietal sulcus, the caudate nucleus, the thalamus, the hippocampus, and occipitotemporal areas. These regions are similar to the delay period network in younger adults in our study that used an IFJ seed. Chang et al. (2007) found significant effective connectivity between left anterior caudate and bilateral BA 6 and 44 during the load-dependent delay phase in normal younger adults, further supporting our functional connectivity findings.

Computational models have been proposed to explain how these two regions may function together during the delay period of working memory tasks. For example, it has been suggested that prefrontal cortical-thalamic loops act to sustain activity in prefrontal neurons during delay periods (Ashby et al., 2005). Specifically, prefrontal cortex excites the head of the caudate nucleus, causing disinhibition of the thalamus and reverberation of activity in these prefrontal cortical-thalamic loops. Bamford and colleagues (2004) have suggested that dopamine acts on these corticostriatal synaptic connections to strengthen the activity of the most active connections by filtering out less active inputs.

Only a few studies have directly investigated how dopamine modulates functional connectivity. Nagano-Saito et al. (2008) found that dopamine depletion resulted in an impairment of frontal-striatal functional connectivity during the Wisconsin Card Sorting Task in normal younger adults. Participants who were not dopamine-depleted showed significant frontal-striatal functional connectivity that was related to faster response times, suggesting that normal dopamine function supports both corticostriatal functional connectivity and efficient task performance. In another study focused on normal older adults

(Honey et al., 2003), participants who were given the D2 antagonist sulpiride had increased functional connectivity in the cortico-striato-thalamic system. These differing results of dopamine on connectivity in older and younger participants are consistent with our results indicating that age-related changes in the dopamine system affect connectivity.

Although the association between higher FMT signal and decreased functional connectivity is correlational, and therefore the directionality of the relationship cannot be determined, the most likely explanation for this relationship is that the age-related loss of dopaminergic neurons causes an upregulation of dopamine synthesis, which may or may not successfully compensate for deficits elsewhere in the dopamine system. It is possible that this upregulation results in non-optimal levels of caudate dopamine, or levels that remain suboptimal. While this hypothesis fits with other studies that have shown similar relationships between these variables (Braskie et al., 2008; Honey et al., 2003), further studies could more clearly specify the relationship between functional connectivity and dopamine, and functional connectivity and task performance, especially in older adults. It will ultimately be important to understand how these steady-state measures of dopamine synthesis relate to synaptic dopamine, which can potentially be explored using a variety of techniques such as methylphenidate challenge with  $^{11}\text{C}$ -raclopride. Investigation of the complex relationships between dopamine synthesis, dopamine release, and brain activity, along with discovery of how these relationships are altered in aging will require multiple experiments to elucidate.

## Supplementary Material

Refer to Web version on PubMed Central for supplementary material.

## Acknowledgments

This study was supported by NIH grant AG027984 to W.J. Jagust. This research was conducted with the approval of the Institutional Review Board of UC Berkeley and Lawrence Berkeley National Laboratory.

## References

- Alexander GE, Crutcher MD. Functional architecture of basal ganglia circuits: neural substrates of parallel processing. *Trends Neurosci.* 1990; 13:266–271. [PubMed: 1695401]
- Alexander GE, DeLong MR, Strick PL. Parallel organization of functionally segregated circuits linking basal ganglia and cortex. *Annu Rev Neurosci.* 1986; 9:357–381. [PubMed: 3085570]
- Ashby FG, Ell SW, Valentin VV, Casale MB. FROST: a distributed neurocomputational model of working memory maintenance. *J. Cog. Neurosci.* 2005; 17:1728–1743.
- Backman L, Ginovart N, Dixon RA, Wahlin TB, Wahlin A, Halldin C, Farde L. Age-related cognitive deficits mediated by changes in the striatal dopamine system. *Am. J. Psychiatry.* 2000; 157:635–637. [PubMed: 10739428]
- Backman L, Karlsson S, Fischer H, Karlsson P, Brehmer Y, Rieckmann A, MacDonald SWS, Farde L, Nyberg L. Dopamine D1 receptors and age differences in brain activation during spatial working memory. *Neurobiol. Aging.* 2009 [published online ahead of print December 3].
- Backman L, Lindenberger U, Li S, Nyberg L. Linking cognitive aging to alterations in dopamine neurotransmitter functioning: Recent data and future avenues. *Neurosci. Biobehav. Rev.* 2010; 34:670–677. [PubMed: 20026186]
- Bamford NS, Zhang H, Schmitz Y, Wu NP, Cepeda C, Levine MS, Schmauss C, Zakharenko SS, Zablow L, Sulzer D. Heterosynaptic dopamine neurotransmission selects sets of corticostriatal terminals. *Neuron.* 2004; 42:653–663. [PubMed: 15157425]
- Braskie MN, Landau SM, Wilcox CE, Taylor SD, O'Neil JP, Baker SL, Madison CM, Jagust WJ. Correlations of striatal dopamine synthesis with default network deactivations during working memory in younger adults. *Hum. Brain Mapp.* 2010 n/a.

- Braskie MN, Wilcox CE, Landau SM, O'Neil JP, Baker SL, Madison CM, Kluth JT, Jagust WJ. Relationship of striatal dopamine synthesis capacity to age and cognition. *J. Neurosci.* 2008; 28:14320–14328. [PubMed: 19109513]
- Brozoski TJ, Brown RM, Rosvold HE, Goldman PS. Cognitive deficit caused by regional depletion of dopamine in prefrontal cortex of rhesus monkey. *Science.* 1979; 205:929–932. [PubMed: 112679]
- Cabeza R, Dolcos F, Graham R, Nyberg L. Similarities and differences in the neural correlates of episodic memory retrieval and working memory. *Neuroimage.* 2002; 16:317–330. [PubMed: 12030819]
- Chang C, Crottaz-Herbette S, Menon V. Temporal dynamics of basal ganglia response and connectivity during verbal working memory. *Neuroimage.* 2007; 34:1253–1269. [PubMed: 17175179]
- Cools R, Sheridan M, Jacobs E, D'Esposito M. Impulsive personality predicts dopamine-dependent changes in frontostriatal activity during component processes of working memory. *J. Neurosci.* 2007; 27:5506–5514. [PubMed: 17507572]
- DeJesus OT, Flores LG, Roberts AD, Dick DW, Bartlett RM, Murali D, Nickles RJ. Aromatic L-amino acid decarboxylase (AAAD) activity in rhesus macaque striatum after MAO-B inhibition by Ro 16–6491. *Synapse.* 2005; 56:54–56. [PubMed: 15700282]
- Dolcos F, Rice HJ, Cabeza R. Hemispheric asymmetry and aging: right hemisphere decline or asymmetry reduction. *Neurosci. Behav. R.* 2002; 26:819–825.
- Erixon-Lindroth N, Farde L, Wahlin TB, Sovago J, Halldin C, Backman L. The role of the striatal dopamine transporter in cognitive aging. *Psychiatry Res.* 2005; 138:1–12. [PubMed: 15708296]
- Fearnley JM, Lees AJ. Ageing and Parkinson's disease: substantia nigra regional selectivity. *Brain.* 1991; 114:2283–2301. [PubMed: 1933245]
- Fiebach CJ, Rissman J, D'Esposito M. Modulation of inferotemporal cortex activation during verbal working memory maintenance. *Neuron.* 2006; 51:251–261. [PubMed: 16846859]
- Frey KA, Koeppe RA, Kilbourn MR, Vander Borgh T, Albin RL, Gilman S, Kuhl DE. Presynaptic monoaminergic vesicles in Parkinson's disease and normal aging. *Ann. Neurol.* 1996; 40:873–884. [PubMed: 9007092]
- Gazzaley A, Rissman J, D'Esposito M. Functional connectivity during working memory maintenance. *Cogn. Affect. Behav. Neurosci.* 2004; 4:580–599. [PubMed: 15849899]
- Gunning-Dixon FM, Head D, McQuain J, Acker JD, Raz N. Differential aging of the human striatum: a prospective MR imaging study. *Am. J. Neuroradiol.* 1998; 19:1501–1507. [PubMed: 9763385]
- Hester R, Garavan H. Executive dysfunction in cocaine addiction: evidence for discordant frontal, cingulate, and cerebellar activity. *J. Neurosci.* 2004; 24:11017–11022. [PubMed: 15590917]
- Honey GD, Suckling J, Zelaya F, Long C, Routledge C, Jackson S, Ng V, Fletcher PC, Williams SCR, Brown J, Bullmore ET. Dopaminergic drug effects on physiological connectivity in a human cortico-striato-thalamic system. *Brain.* 2003; 126:1767–1781. [PubMed: 12805106]
- Jordan S, Eberling JL, Bankiewicz KS, Rosenberg D, Coxson PG, VanBrocklin HF, O'Neil JP, Emborg ME, Jagust WJ. 6-[18F]fluoro-L-m-tyrosine: metabolism, positron emission tomography kinetics, and 1-methyl-4-phenyl-1,2,3,6-tetrahydropyridine lesions in primates. *Brain Res.* 1997; 750:264–276. [PubMed: 9098552]
- Kaasinen V, Vilkmann H, Hietala J, Nägren K, Helenius H, Olsson H, Farde L, Rinne JO. Age-related dopamine D2/D3 receptor loss in extrastriatal regions of the human brain. *Neurobiol. Aging.* 2000; 21:683–688. [PubMed: 11016537]
- Kish SJ, Zhong XH, Hornykiewicz O, Haycock JW. Striatal 3,4-dihydroxyphenylalanine decarboxylase in aging: disparity between postmortem and positron emission tomography studies? *Ann. Neurol.* 1995; 38:260–264. [PubMed: 7654075]
- Landau SM, Lal R, O'Neil JP, Baker S, Jagust WJ. Striatal dopamine and working memory. *Cereb. Cortex.* 2009; 19:445–454. [PubMed: 18550595]
- Lehericy S, Ducros M, Van de Moortele PF, Francois C, Thivard L, Poupon C, Swindale N, Ugurbil K, Kim D. Diffusion tensor fiber tracking shows distinct corticostriatal circuits in humans. *Ann. Neurol.* 2004; 55:522–529. [PubMed: 15048891]

- Ma SY, Royttat M, Collant Y, Rinne JO. Unbiased morphometrical measurements show loss of pigmented nigral neurones with ageing. *Neuropathol. Appl. Neurobiol.* 1999; 25:394–399. [PubMed: 10564529]
- Meltzer CC, Kinahan PE, Greer PJ, Nichols TE, Comtat C, Cantwell MN, Lin MP, Price J. Comparative evaluation of MR-based partial-volume correction schemes for PET. *J. Nucl. Med.* 1999; 40:2053–2065. [PubMed: 10616886]
- Middleton FA, Strick PL. Basal ganglia and cerebellar loops: motor and cognitive circuits. *Brain Res. Rev.* 2000; 31:236–250. [PubMed: 10719151]
- Nagano-Saito A, Leyton M, Monchi O, Goldberg YK, He Y, Dagher A. Dopamine depletion impairs frontostriatal functional connectivity during a set-shifting task. *J. Neurosci.* 2008; 28:3697–3706. [PubMed: 18385328]
- Nagel IE, Preuschhoff C, Li S, Nyberg L, Backman L, Lindenberger U, Heekeren HR. Performance level modulates adult age differences in brain activation during spatial working memory. *Proc. Natl. Acad. Sci.* 2010; 106:22552–22557. [PubMed: 20018709]
- Noll, DC.; Stenger, VA.; Vazquez, AL.; Peltier, SJ. Spiral scanning in fMRI. In: Moonen, CTW.; Bandettini, PA., editors. *Functional MRI*. New York: Springer-Verlag; 1999. p. 149-160.
- Park, DC.; Hedden, T. Working memory and aging. In: Naveh-Benjamin, M.; Moscovitch, M.; Roediger, HL., editors. *Perspectives on human memory and cognitive aging: Essays in honour of Fergus Craik*. East Sussex: Psychology Press; 2002. p. 148-160.
- Park DC, Smith AD, Lautenschlager G, Earles JL, Frieske D, Zwahr M, Gaines CL. Mediators of long-term memory performance across the life span. *Psychol. Aging.* 1996; 11:621–637. [PubMed: 9000294]
- Patlak CS, Blasberg RG. Graphical evaluation of blood-to-brain transfer constants from multiple-time uptake data: generalizations. *J. Cereb. Blood Flow Metab.* 1985; 5:584–590. [PubMed: 4055928]
- Ranganath C, Heller A, Cohen MX, Brozinsky CJ, Rissman J. Functional connectivity with the hippocampus during successful memory formation. *Hippocampus.* 2005; 15:997–1005. [PubMed: 16281291]
- Raz N, Gunning FM, Head D, Dupuis JH, McQuain J, Briggs SD, Loken WJ, Thornton AE, Acker JD. Selective aging of the human cerebral cortex observed in vivo: differential vulnerability of the prefrontal grey matter. *Cereb. Cortex.* 1997; 7:268–282. [PubMed: 9143446]
- Raz N, Rodrigue KM, Kennedy KM, Head D, Gunning-Dixon F, Acker JD. Differential aging of the human striatum: longitudinal evidence. *Am. J. Neuroradiol.* 2003; 24:1849–1856. [PubMed: 14561615]
- Reuter-Lorenz PA. New visions of the aging mind and brain. *Trends Cogn. Sci.* 2002; 6:394–400. [PubMed: 12200182]
- Reuter-Lorenz, PA.; Sylvester, CC. The cognitive neuroscience of working memory and aging. In: Cabeza, R., editor. *Cognitive Neuroscience of Aging: Linking Cognitive and Cerebral Aging*. Oxford UP: Cary; p. 186-215.
- Rinne JO, Lonnberg P, Marjamaki P. Age-dependent decline in human brain dopamine D1 and D2 receptors. *Brain Res.* 1990; 508:349–352. [PubMed: 2407314]
- Rissman J, Gazzaley A, D'Esposito M. Measuring functional connectivity during distinct stages of a cognitive task. *Neuroimage.* 2004; 23:752–763. [PubMed: 15488425]
- Rypma B, D'Esposito M. Age-related changes in brain-behavior relationships: evidence from event-related functional MRI studies. *Eur. J. Cognit. Psychol.* 2001; 13:235–256.
- Seeman P, Bzowej NH, Guan HC, Bergeron C, Becker LE, Renyolds GP, Bird ED, Riederer P, Jellinger L, Wantanabe S, Tourtelletotte WW. Human brain dopamine receptors in children and aging adults. *Synapse.* 1987; 1:399–404. [PubMed: 3505371]
- Severson JA, Marcusson J, Winblad B, Finch CE. Age-correlated loss of dopaminergic binding sites in human basal ganglia. *J. Neurochem.* 1982; 39:1623–1631. [PubMed: 7142992]
- Sternberg S. High-speed scanning in human memory. *Science.* 1966; 153:652–654. [PubMed: 5939936]
- Tomasi D, Volkow ND, Wang R, Telang F, Wang GJ, Chang L, Ernst T, Fowler JS. Dopamine transporters in striatum correlate with deactivation in the default mode network during visuospatial attention. *PLoS One.* 2009; 4:e6102. [PubMed: 19564918]

- VanBrocklin HF, Blagoev M, Hoeppeing A, O'Neil JP, Klose M, Schubiger PA, Ametamey S. A new precursor for the preparation of 6-[18F]Fluoro-L-m-tyrosine ([18F]FMT): efficient synthesis and comparison of radiolabeling. *Appl. Radiat. Isot.* 2004; 61:1289–1294. [PubMed: 15388123]
- Volkow ND, Fowler JS, Wang GJ, Logan J, Schlyer D, MacGregor R, Hitzemann R, Wolf AP. Decreased dopamine transporters with age in healthy human subjects. *Ann. Neurol.* 1994; 36:237–239. [PubMed: 8053661]
- Williams GV, Goldman-Rakic PS. Modulation of memory fields by dopamine D1 receptors in prefrontal cortex. *Nature.* 1995; 376:572–575. [PubMed: 7637804]
- Wolf ME, LeWitt PA, Bannon MJ, Dragovic LJ, Kapatos G. Effect of aging on tyrosine hydroxylase protein content and the relative number of dopamine nerve terminals in human caudate. *J. Neurochem.* 1991; 56:1191–1200. [PubMed: 1672141]
- Yoon JH, Curtis CE, D'Esposito M. Differential effects of distraction during working memory on delay-period activity in the prefrontal cortex and the visual association cortex. *Neuroimage.* 2006; 29:1117–1126. [PubMed: 16226895]
- Zhang Y, Brady M, Smith S. Segmentation of brain MR images through a hidden Markov random field model and the expectation-maximization algorithm. *IEEE Trans. Med. Imaging.* 2001; 20:45–57. [PubMed: 11293691]

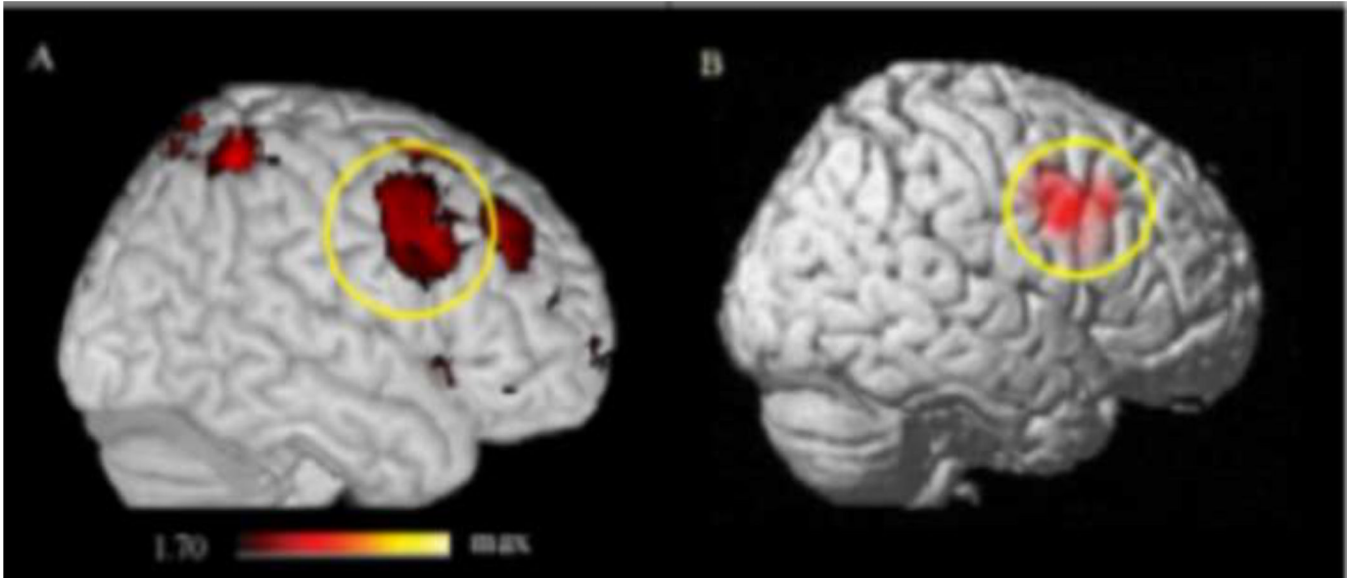


**Figure 1.**

A) Right BA 44/6 activity ( $x=64, y=18, z=32$ ) in the load-dependent delay contrast (high load delay period > low load delay period) for all participants (displayed at  $p<0.05$ , for illustrative purposes). B) All participants' right BA 44/6 seed regions used for connectivity analysis simultaneously overlaid on the standard brain (darker red indicates a greater degree of overlap).

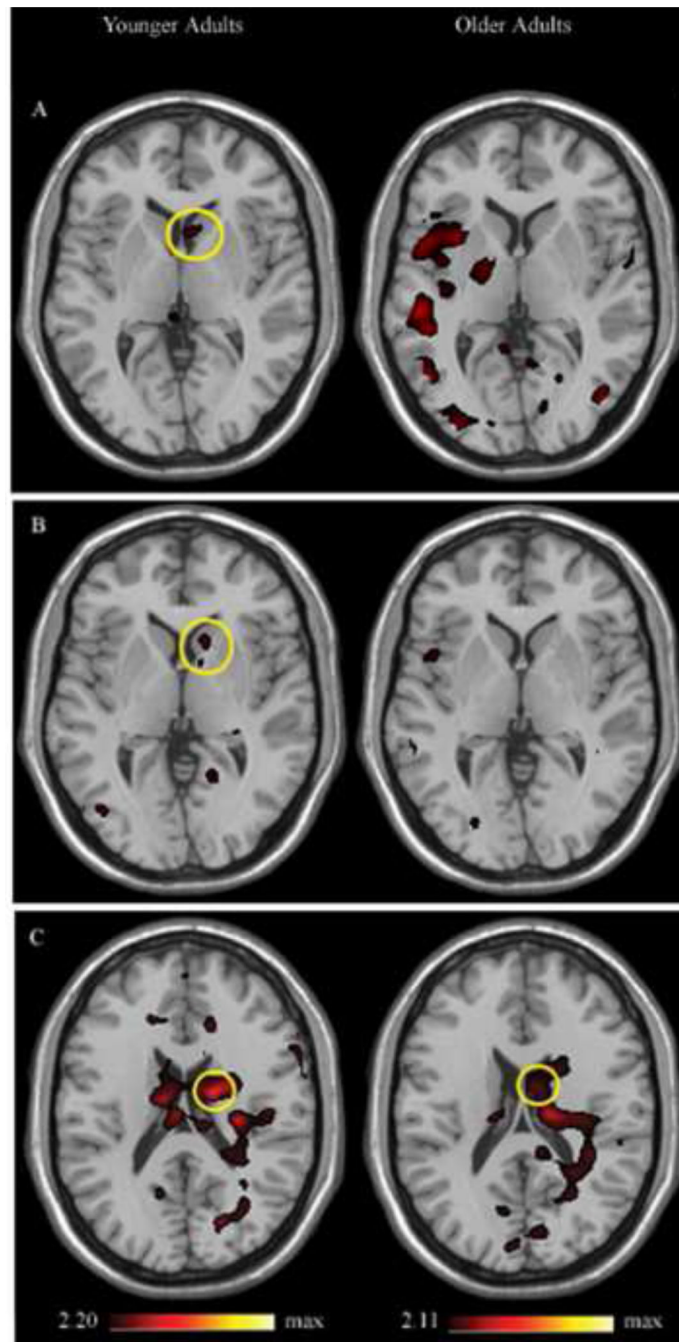


**Figure 2.** Functional connectivity between right BA 44/6 and the right caudate in younger and older adults during the load-dependent a) encoding period, b) delay period, and c) response period.

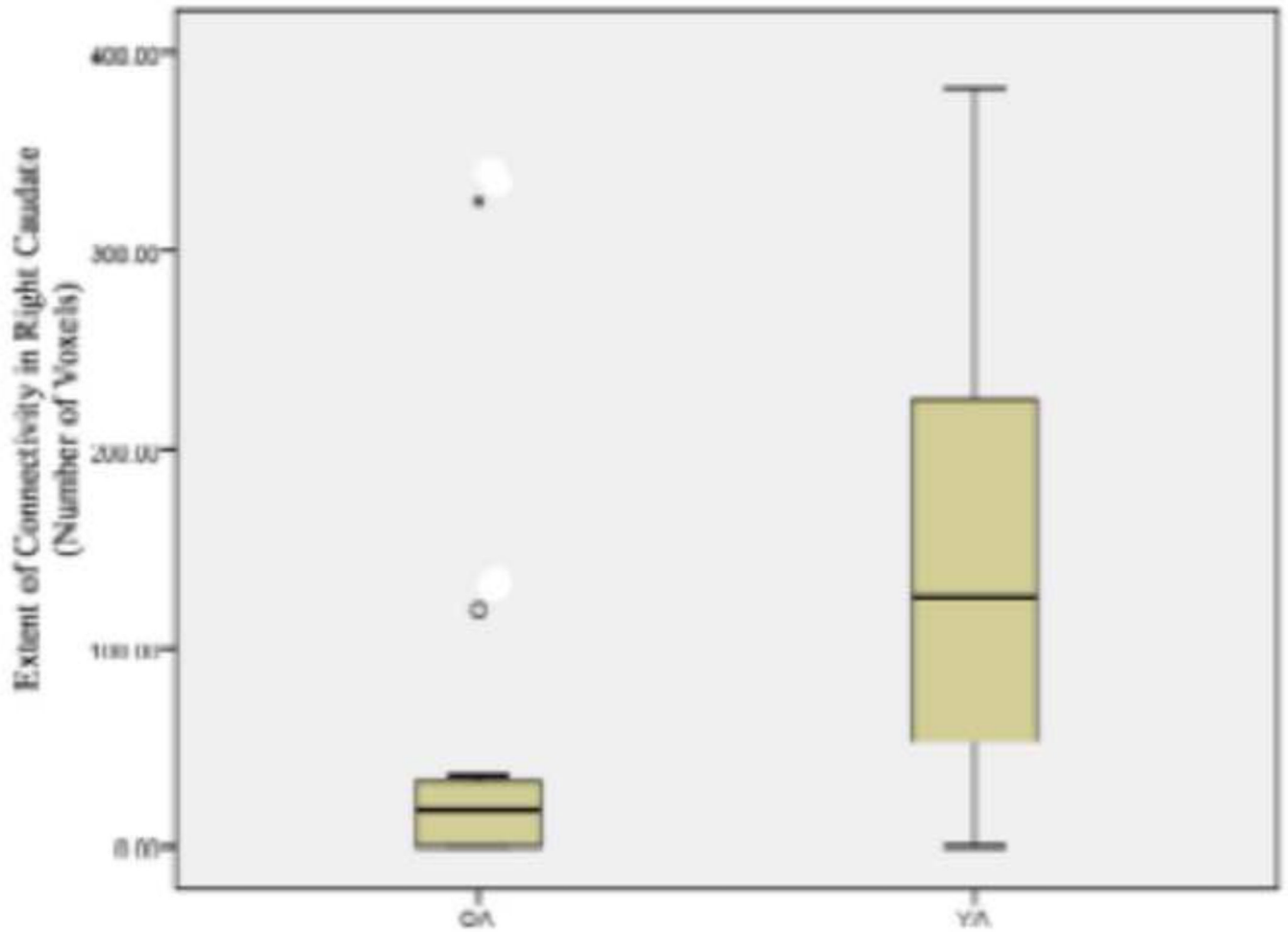


**Figure 3.** The extent of functional connectivity during the load-dependent delay period in the right caudate is significantly greater for younger adults (YA) than older adults (OA) ( $t(28) = -2.972, p < 0.006$ ).



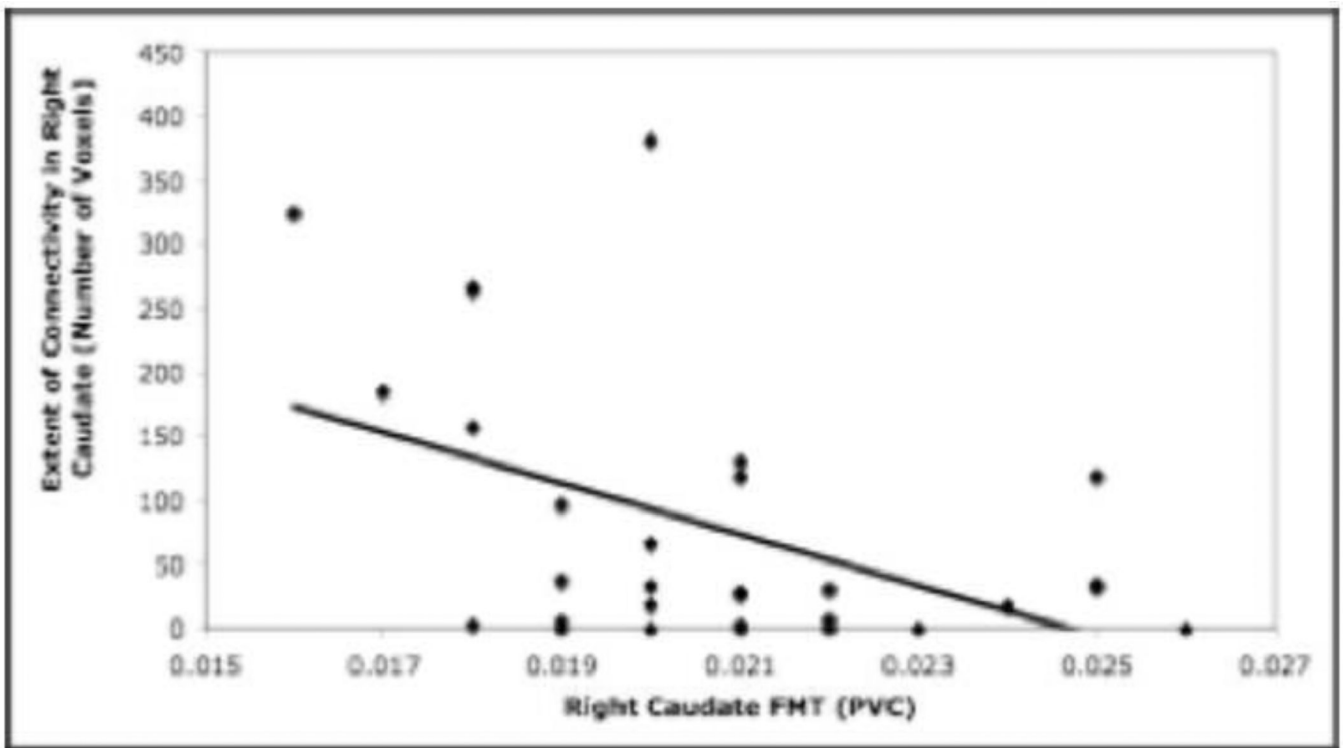


**Figure 4.** The extent of connectivity in the right caudate during the load-dependent delay period is significantly negatively correlated with right caudate FMT across the two age groups ( $r = -0.472$ ,  $p < 0.01$ ).

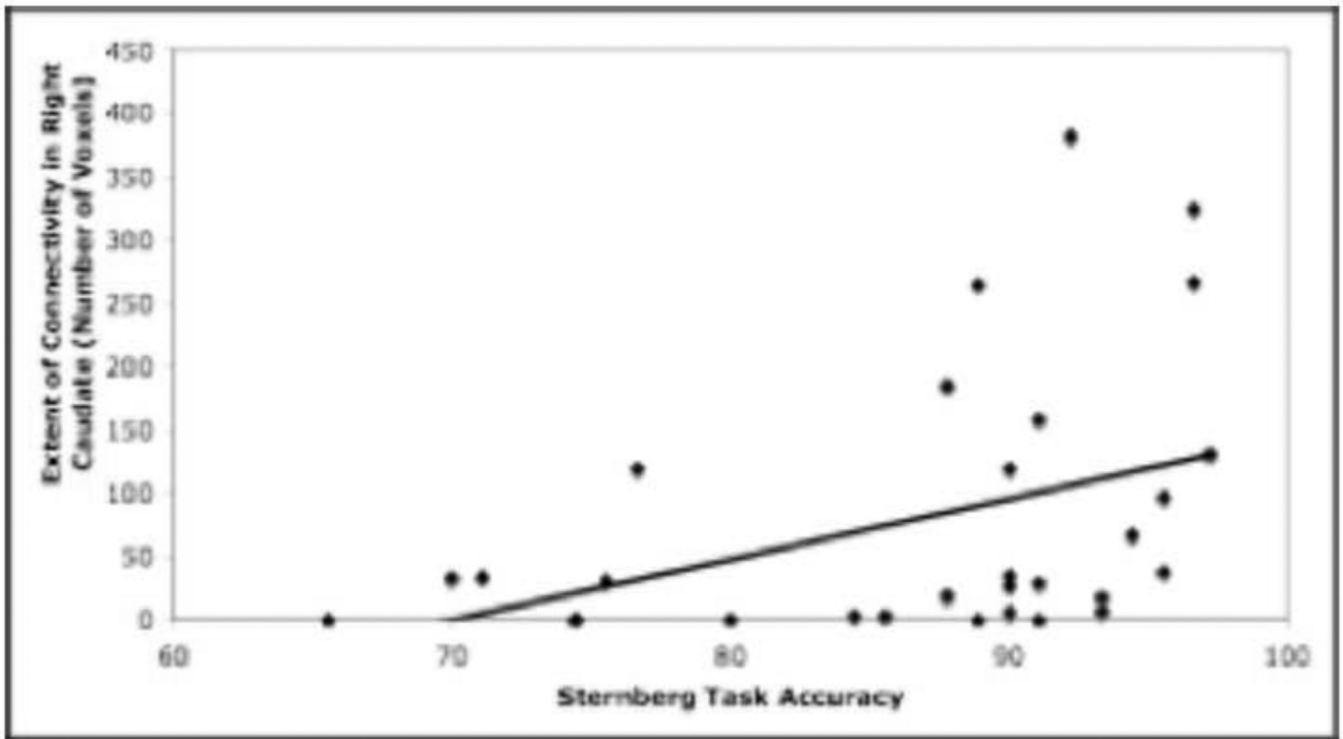


**Figure 5.** The extent of connectivity in the right caudate during the load-dependent delay period is significantly positively correlated with accuracy (percent correct) on the Sternberg working memory task ( $r= 0.400$ ,  $p<0.05$ ).

**Table 1**

## Demographic Characteristics and Task Performance

	<b>Younger Adults</b>	<b>Older Adults</b>
Number of Participants	12	18
Age (Years) # *	22.7 ± 2.77	64.78 ± 5.57
Sex	9 Female; 3 Male	12 Female; 6 Male
Years of Education # *	15.75 ± 1.22	18.56 ± 2.18
MMSE #	29.25 ± 0.87	29.50 ± 0.71
Sternberg Task Accuracy # +	90.14 ± 6.66	84.32 ± 9.62
Sternberg Task Reaction Time # *	1085.86 ± 297.59	1235.06 ± 308.40
Right Caudate FMT # *	0.019 ± .002	0.022 ± 0.002
Left Caudate FMT # *	0.019 ± .002	0.022 ± 0.003

# Listed as mean ± standard deviation

\* Indicates a significant difference between the older adult group and the younger adult group ( $p < 0.05$ )

+ Indicates a trend for significance between the older adult and younger adult group ( $p = 0.079$ )